

RESEARCH

Open Access



Application of Frictional Bond-Slip Model to Large-Scale FRP-Strengthened T-Beams with U-wraps

Jaeha Lee^{1*}  and Maria Lopez²

Abstract

Studies on U-wraps generally focus on the experimental results and mechanisms of the shear strengthening effect. Only a few studies have focused on the anchoring effect of the longitudinal FRP due to addition of the U-wrap. Lee and Lopez (*Constr Build Mater* 194:226–237, 2016) have found experimentally from pull-out tests that incremental changes occur in the debonding strain at the concrete-FRP interface depending on the various type of U-wraps. The proposed numerical method using the Frictional Bond-Slip (FBS) model has been validated by comparing the pull-out test results (Lee and Lopez *Constr Build Mater* 194:226–237, 2016). In the present study, the FBS model was applied to characterize the behavior of a large scale FRP strengthened T-beam with multiple U-wraps. First, the 2-dimensional (2D) model for pull-out test was developed. Debonding load and behavior of the model were compared with both the experimental results (Lee and Lopez *Constr Build Mater* 194:226–237, 2016) and the simulation results of a 3-dimensional (3D) model from a previous study (Lee and Lopez *Constr Build Mater* 194:226–237, 2016). Next, the 2D model was applied to model the behavior of a large scale FRP strengthened T-beam with multiple U-wraps. The conducted 2D simulation using the proposed FBS model predicted well the strains at various locations on the FRP sheet, the flexural capacity and complex failure mode of the FRP strengthened beam with several U-wraps. The proposed FBS model was also applied to other comparable studies, and debonding strains were successfully predicted within an margin of error of 7%. Using the validated model, a parametric study of the FRP strengthened T-beam was conducted with various key parameters of the U-wrap, such as the angle of U-wrap and the number of U-wrap.

Keywords: FRP U-wrap, beam test, FRP debonding, anchor effect, frictional behavior

1 Introduction

In order to prevent debonding failure of concrete-FRP interfaces, several different types of new anchoring systems for externally bonded FRP applications have been introduced (e.g. Zhang and Smith 2012; Lee et al. 2009; Ozbakkaloglu and Saatcioglu 2009; Triantafillou 1998; Grelle and Sneed 2013). These developed anchor systems include fiber type, mechanical types, U-wrap (three sides) and metal rod types. Among these anchoring systems,

the U-wraps have received large attention because of several advantages they offer, such as shear strengthening and anchoring effect. Furthermore, the same material with the FRP sheet can also be used as U-wrap, indicating that the preoperational steps for installing the anchoring system can be reduced. The other benefits of choosing U-wrap are well described in Lee and Lopez's previous research work (Lee and Lopez 2016; Lee 2010), Brena et al. (2003) and Khalifa and Al-Tersawy (2013).

Past research (Lee and Lopez, 2016) reported experimentally that frictional behavior between the debonded surfaces of concrete and FRP sheet is a key factor to control the anchoring effect of the FRP U-wrap. Obtained basic material properties such as concrete

*Correspondence: jaeha@kmou.ac.kr

¹ Department of Civil Engineering, National Korea Maritime and Ocean University, 609 Engineering Building-II, Busan 606-791, South Korea
Full list of author information is available at the end of the article
Journal information: ISSN 1976-0485 / eISSN 2234-1315

tensile and compressive strength, tensile strength of concrete-epoxy interface, transverse tensile properties of FRP sheet and epoxy, shear properties of unidirectional FRP sheet were obtained according to ASTM standards (2005, 2011, 2012, 2014) and well summarized in Lee and Lopez (2016). The observed friction between a FRP sheet and the surface of the concrete in the U-wrap region has been incorporated into an interfacial model which predicts the debonding strain of the FRP sheet under the U-wrap(s). It is the frictional bond-slip (FBS) model which was used to satisfactorily predict the debonding failure in the U-wrap region and the residual strength of the U-wrap after debonding failure against the pull-out loadings in a three-dimensional (3D) space (Lee and Lopez 2019). The anchoring effects were verified by Lee and Lopez (2016) through the experimental studies, where most of the U-wrap pull-out specimens showed higher debonding strains than the strains predicted from Chen and Teng's equations (2001). Since the equations by Chen and Teng (2001) for prediction of debonding strain were developed under the pull-out loading conditions without any U-wraps and widely accepted for the prediction of FRP debonding strain, this result indicated that there was a certain amount of anchoring effect from the U-wraps. However, there was a limited study regarding a FBS model (Lee and Lopez 2019) which has been only applied to the concrete block with an attached FRP sheet under pull-out loading condition. To note, the U-wrap is mainly applied to the surface of girders (beam) rather than a simple concrete block, as shown in Fig. 1. Therefore, the application of the FBS model

to practical structures such as large-scaled T-beams is worth studying.

In the present study, the FBS model which was originally developed based on 3D has been investigated for beam applications. First, 2D applications were investigated since the 2D beam analysis is normally more preferred due to its simplicity, applicability and computational efficiency, especially for beams. Therefore, a 2D model for pull-out test was developed and debonding behavior of the model was compared with experimental data and results from 3D model for verification purposes (Lee and Lopez 2019). Next, a T-beam with U-wrap was modelled using the FBS model. Load-displacement graphs, strain distributions along the length of the FRP and local strain data from some of the U-wraps were compared with the experimental data. The debonding strain of longitudinal FRP sheet was also compared with the experimental data. Finally, using the developed 2D FBS model for beam applications, parametric studies were done with key parameters such as the number of U-wraps and the angle of the U-wraps, their effects were explored on the flexural behavior of the T-beam.

2 Application of the Frictional Bond Slip (FBS) Model for T-beam

In the present work, the FBS model was developed based on the experiments by Lee and Lopez (2016) on pull-out test with U-wraps. On applying the newly developed FBS model, the strengthening effects of anchoring under the pulling out loading could be satisfactorily predicted. The behavior of concrete-epoxy interface (CEI) under the U-wrap region (see Fig. 2) had been described well by Lee

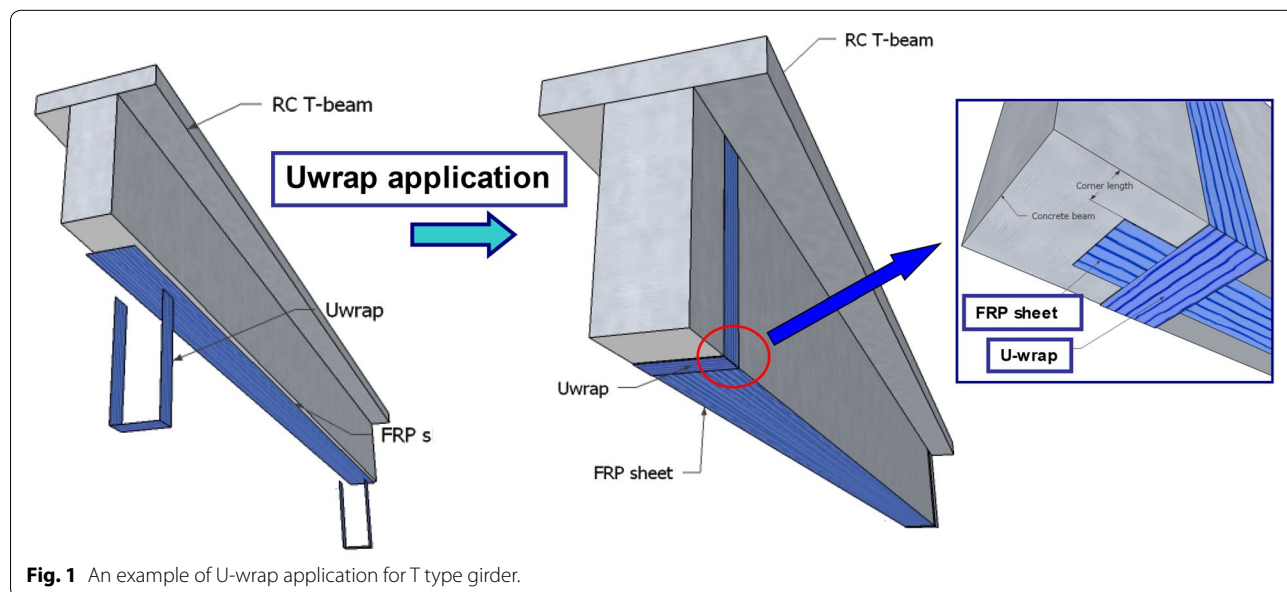


Fig. 1 An example of U-wrap application for T type girder.

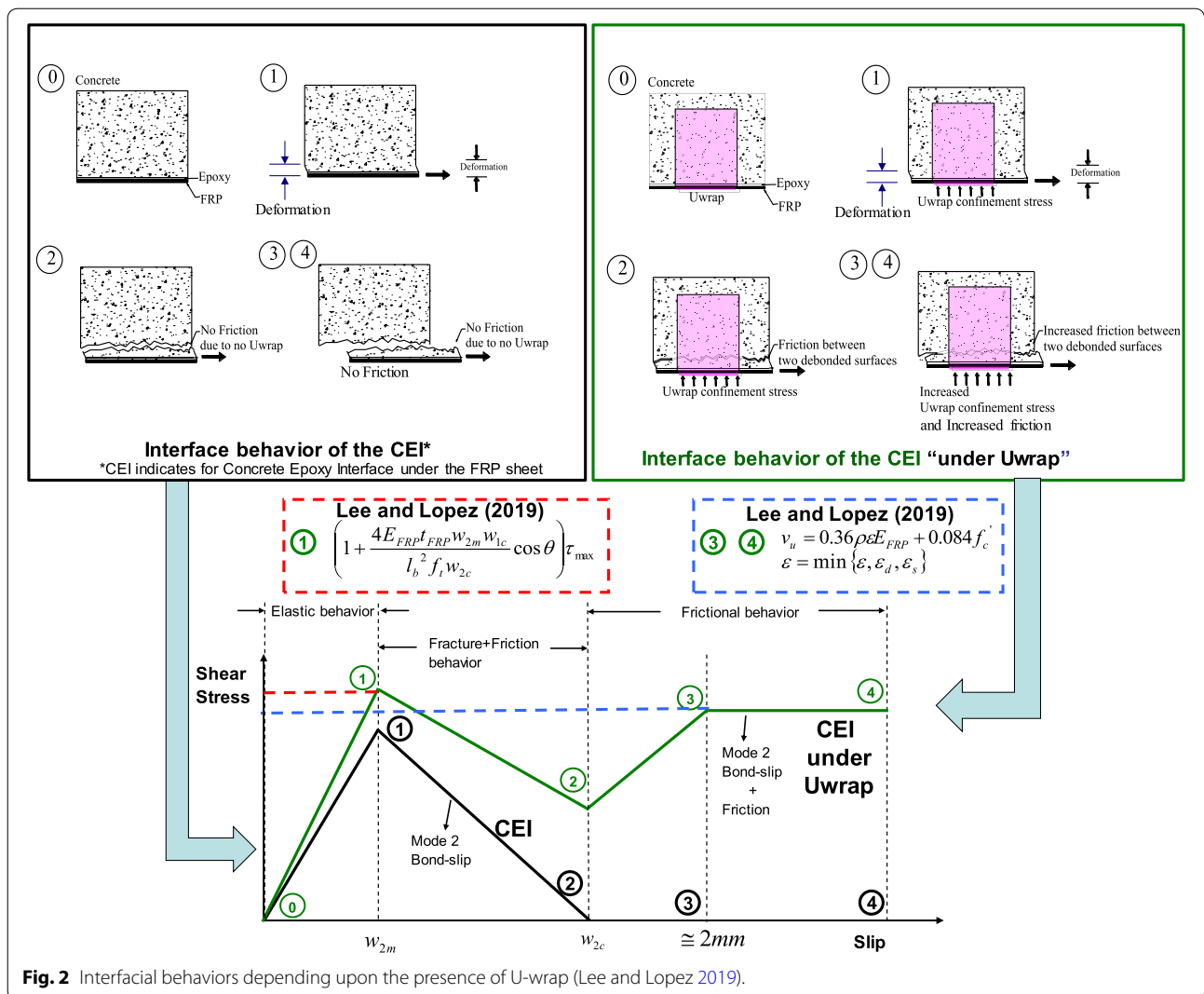


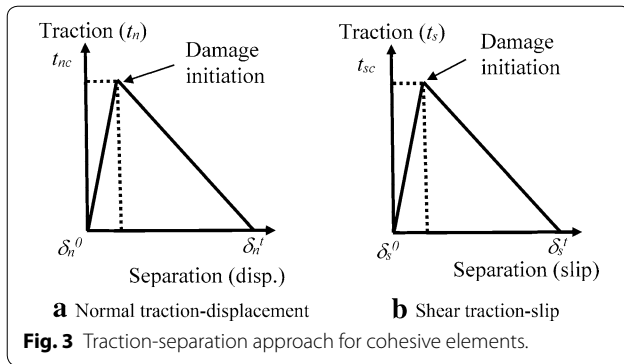
Fig. 2 Interfacial behaviors depending upon the presence of U-wrap (Lee and Lopez 2019).

and Lopez using the FBS model (2019). A key parameter to determine each point of the graph in Fig. 2 is pressure from confinement stress of U-wrap generated by deformation of the interface. In Fig. 2, if there was no U-wrap, no confinement stress would be generated; consequently, no frictional behavior would occur. On the other hand, if U-wrap exists, confinement stress will generate and frictional slip between the two debonded surfaces will be a key factor to delay the debonding failure of the externally bonded FRP strengthened elements. Detailed information on FBS model and calculations for each point that are shown in Fig. 2 can be found in Lee and Lopez (2019).

3 Application of the FBS Model in 2D Beam Modeling Using Cohesive Elements

The four points of the FBS model shown in Fig. 2 represented the Mode 2 interfacial behavior in the region of the U-wrap (Lee and Lopez 2019). Mode 2 interfacial

behavior indicates traction–separation (slip) deformation. Likewise, Mode 1 interfacial behavior can also be described as traction–separation (normal displacement). The detailed explanation has been illustrated in Fig. 3. Accordingly, the FBS curves shown in Fig. 2 can be incorporated into the cohesive elements (e.g. Hibbitt et al. 2017) of Abaqus in the U-wrap region as material properties. The cohesive elements can be used in large displacement analysis since these elements undergo finite displacement (Hibbitt et al. 2017). Since there are large displacements (slips) between an FRP sheet and a concrete beam due to anchoring effects, as the FBS model shows (see Fig. 2), application of the cohesive element between two debonded surfaces could be a proper option. The cohesive elements can be applied for modeling bonded interfaces. Both the continuum approach and the traction–separation approach can be used for constitutive response of the cohesive elements. In the



current study, the traction–separation approach has been utilized since the interface between the FRP sheet and concrete beam can be considered to be of negligible thickness and the FBS model shown in Fig. 2 can be simply described as a traction–separation form.

The cohesive element offers a variety of advantages for applications into the concrete–FRP interfacial behavior. A delamination between the concrete and FRP can be characterized and the Mode 1 and Mode 2 damage behavior (fracture mechanics) can be put into one element as shown in Fig. 3. In other words, the cohesive element can behave in both the normal and shear directions. Furthermore, the frictional part of the FBS model can be characterized as tabulating the experimental data into the input files. However, non-linear behavior until the onset of damage is not possible for this element as the constitutive law for this element is shown in Eq. 1. This linear traction–separation law before the onset of damage can be written as shown in Eq. 1.

$$\begin{Bmatrix} t_n \\ t_s \\ t_t \end{Bmatrix} = \begin{bmatrix} E_{nn} & E_{ns} & E_{nt} \\ E_{ns} & E_{ss} & E_{st} \\ E_{nt} & E_{st} & E_{tt} \end{bmatrix} \begin{Bmatrix} \varepsilon_n \\ \varepsilon_s \\ \varepsilon_t \end{Bmatrix} \quad (1)$$

where, t : Nominal stress (n : normal traction stress, s, t : shear traction stress), E : Modulus that relates stress to strain, ε : Strain.

For uncoupled behavior, all shear components in the matrix vanished. In our present study, An uncoupled behavior and a quadratic equation were used to define damage initiations after conducting a parametric study considering the coupling effect.

Once it reached the maximum stress, the material began to degrade, as shown in Fig. 3. To deal with this softening behavior, the damage variable (D) was applied to the cohesive elements. The relation between the damage variable and stress for both direction are defined in Eq. 2 and 3.

$$t_n = (1 - D)t_{nc} \quad (2)$$

$$t_s = (1 - D)t_{sc} \quad (3)$$

where, t_n : Nominal stress in normal direction, t_s : Shear stress in shear direction, t_{nc} : Maximum nominal stress in normal direction, t_{sc} : Maximum shear stress in normal direction, D : Damage variable.

More detailed information on the cohesive element and applications of Mode 1 and Mode 2 mixed mode fracture energy into the interface properties can be found in previously published papers (e.g. Yuan et al. 2004; Lee et al. 2010; Kishi et al. 2005; Niu et al. 2006; Wang 2007; Wang and Zhang 2008; Kotynia et al. 2008; Baky et al. 2012; Hibbitt Karlsson and Sorenson Inc 2017).

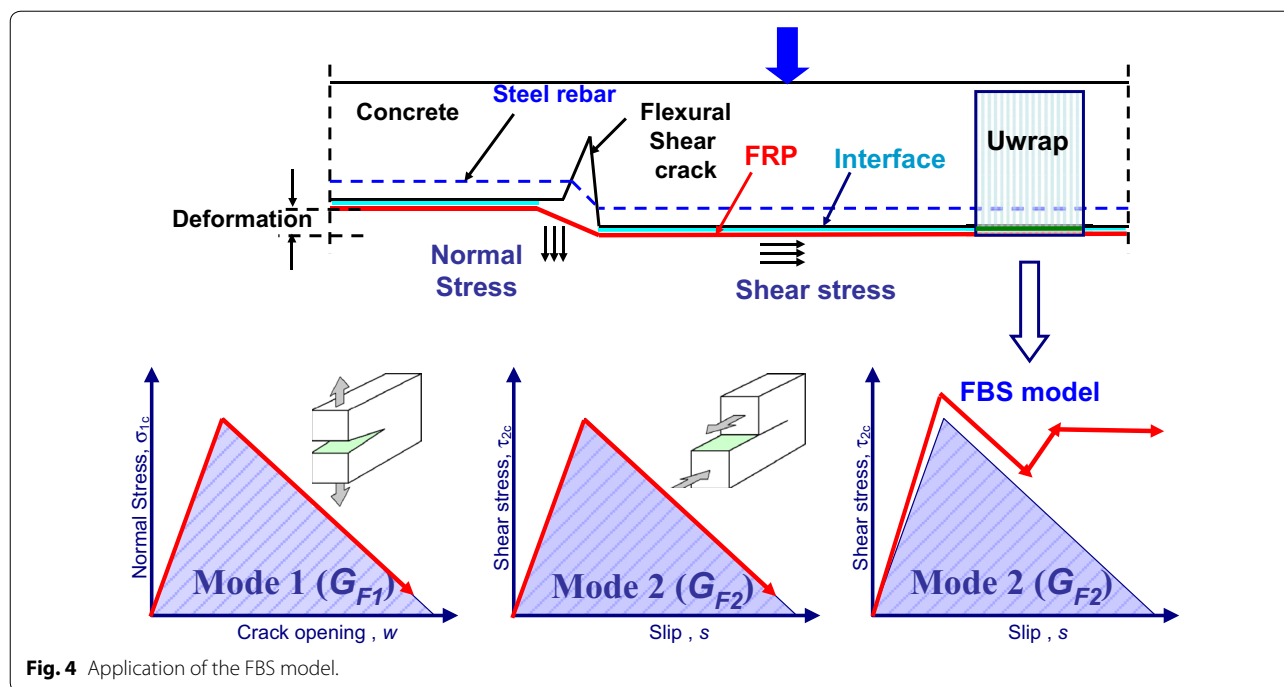
Figure 4 shows the conceptual drawing of the application of the FBS model. An ordinary interface between the concrete and the FRP can be modeled using Mode 1 stress-crack opening (disp.) behavior and Mode 2 shear stress-slip behavior (e.g. Lee et al. 2010). However, in the region of the U-wrap, the interface behavior between concrete and FRP would be affected by the confinement stress generated from the U-wrap, as described in Fig. 2. Therefore, the FBS model should be applied in this region, as shown in Fig. 4. The FBS model was implemented using cohesive element and tabulated input values based on Lee and Lopez (2019).

4 Modeling of the 2D Pull-Out Tests

Based on the previously developed 3D pull-out models (Lee and Lopez 2019), 2D models were developed. A 3D model, especially for beams strengthened with all the U-wraps and FRP sheet, is not an effective model since it requires a large number of elements to cover all the interfaces between the concrete and FRP sheet as well as the interfaces between the concrete and U-wrap. Furthermore, relatively fine mesh should be used for entire concrete body in order to consider cracked section properly. As previously explained, the 3D large scale T-beam model with damage material model might require at least 6,000,000 elements and more than 400 h CPU computational time with a high-performance computer, which has 2.6 GHz processors and 32 GB of ECC ram. Furthermore, a refined element is required for the concrete and interface elements if the cracked region and local behavior of the strengthened beam are the focus rather than the global behavior.

Therefore, developing an effective 2D model of the pull-out test is an important step toward modelling the beam in the present study. This section will show the developed 2D models and comparisons with the results of the developed 3D models of pull-out specimens (Lee and Lopez 2019).

Figure 5 shows the simplified 2D pull-out model developed in the present study and a 3D pull-out models



introduced in Lee and Lopez (2019). First, simplification was taken that the U-wraps attached to both sides of the beams had the same dimensions and same behavior. Therefore, the stiffness of the modeled interface increased by two for considering 3D configuration in 2D. Second, it was assumed that there was a perfect bond in the portion of the U-wrap attached to the longitudinal FRP sheet.

Figure 5 shows a detailed illustration of the developed 2D model for the pullout test. For modeling in 2D, a plain strain element was adopted for the FRP sheet. For the U-wrap in 2D model, a plain stress element was used rather than a plain strain element since the U-wrap was relatively thinner (1.0 mm/one layer) than the width of the FRP sheet and the block of concrete. The interface between the FRP sheet and the concrete was modeled using a 2D cohesive model, in which two types of fracture energies in Mode 1 and Mode 2 directions, as explained previously, were implemented. It was located only between the concrete and FRP sheet. For the interface between the lateral side of the concrete beam and the U-wrap, no cohesive element was used in the 2D models since it was assumed that Mode 1 behavior between the lateral side of the concrete and U-wrap does not exist in the 2D models for simplicity of the model. Therefore, only Mode 2 bond-slip behavior was considered for the concrete-U-wrap connection. The node of the U-wrap element was connected to the nodes of the lateral side of the concrete beam by a connector. The connector was a link

element which uses the Mode 2 constitutive law between the concrete and the FRP. The proposed FBS model was applied to the cohesive element between the concrete and the FRP sheet under the U-wrap region and to link the element at the lateral side of the concrete beam. At the normal interface between the concrete and FRP (no U-wrap region), ordinary bond-slip model was put into the cohesive element as usual using fracture energy. The stress concentration factor was also considered since 2D models cannot generate the stress concentration at the corner area. For estimation of stress concentration factor in the corner region, equations by Campione et al. (2001) were used.

5 Verification with the Experimental Data

The results of the 2D model were further compared with the results of the experiments of Lee and Lopez (2016) and the 3D model of Lee and Lopez (2019) for verification. The FBS model was implemented in the cohesive elements used between the FRP and concrete under U-wrap. The load–displacement graphs of the loaded end and slip distribution along the length of the FRP sheet, as estimated by the FBS model (solid line), were compared with the experiment results (dotted line). The developed 2D model with application of the FBS model predicted the increased debonding strength (Fig. 6a, b) and slip profiles of the FRP sheet (Fig. 6c, d) well due to different anchoring configurations and various U-wrap inclinations (angles).

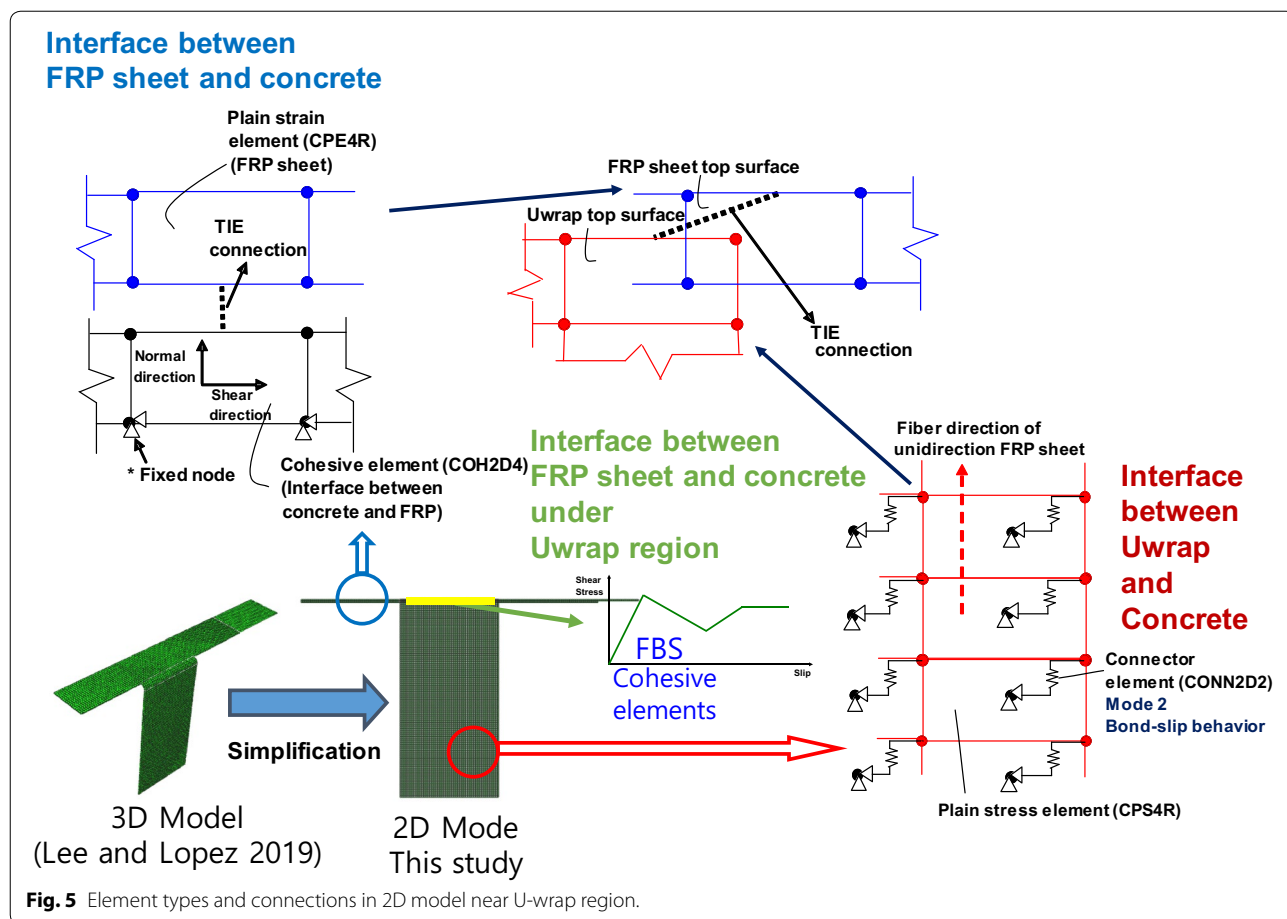


Fig. 5 Element types and connections in 2D model near U-wrap region.

Figure 6a shows comparisons of the load–displacement graph of the 90° U-wrap (90) and 45° U-wrap (45) specimens with the 3D model (Lee and Lopez 2019). The overall trends were similar to each other. However, the 2D models seemed to predict a slightly lower load than the 3D model. Fig. 6b shows the load–displacement graph of the 90° and 45° specimens compared with the experimental results (Lee and Lopez 2019). Figure 6c shows a comparison of slip profile with the 3D model just before the onset of the debonding which is the maximum pull-out load. Fig. 6d shows a comparisons of the slip profile with digital image correlation (DIC) data (Lee and Lopez 2011).

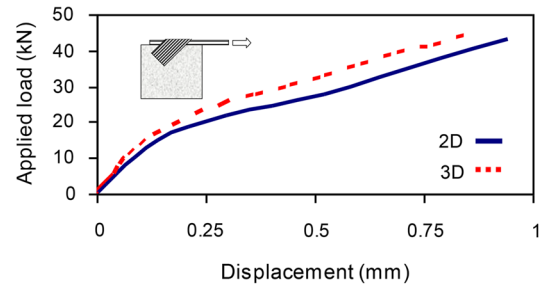
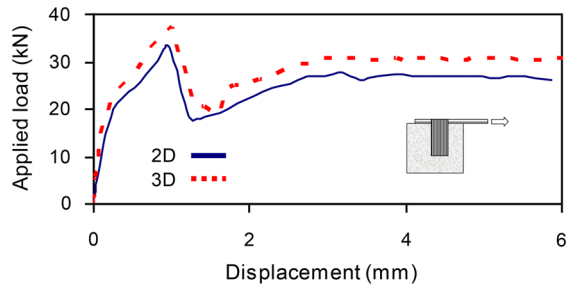
These results showed that the 3D models predicted the behavior of the 90° specimens better than the 2-D model. By contrast, the 2D models were better at predicting the behavior of the 45° specimens. However, it can be concluded that both the models could satisfactorily predict the load–displacement behavior and showed the strengthening effect by friction due to addition of the U-wrap. Based on the obtained results from the 2D model, two assumptions for simplification of the 3D to

the 2D model were adequate. The difference between the 2D and 3D models could be considered as negligible factor, while for conservative design, the 2D model was a better option for the current study.

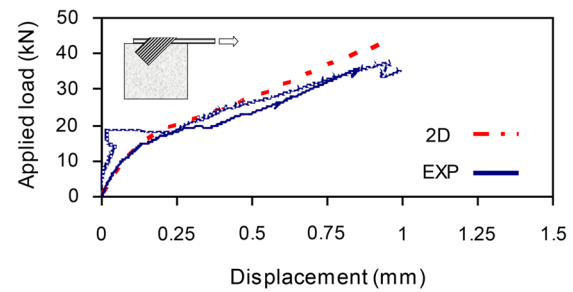
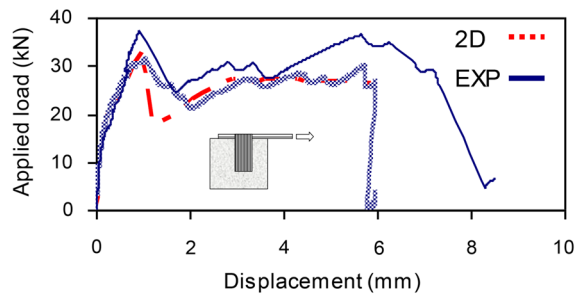
6 Verification of the FBS Model on a Large-scale T Beam

In order to verify the application of the proposed FBS model, a large-scale T-beam was designed and fabricated. To select the geometry of the T-beam, the design was based on typical RC bridge girders from U.S. in the 1950s. The cross-sectional design of the T beam has been shown in Fig. 7. This beam did not have sufficient flexural capacity to meet the current AASHTO LRFD design specification. In order to meet this standard, three layers of CFRP sheet were considered to be applied on its soffit and a tested-T beam was specially designed for the anchor effects, as 45° U-wraps were applied after the application of longitudinal FRP sheet.

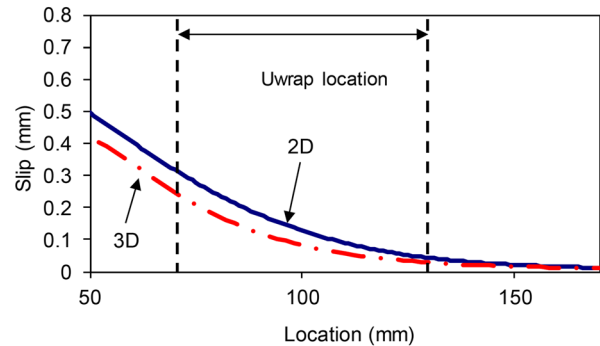
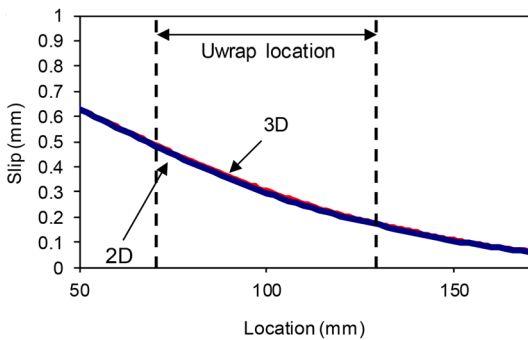
Specific design description for the T-beam itself could be found in Lee et al. (2010), while the FRP strengthening and anchor design using a 45° U-wrap could be



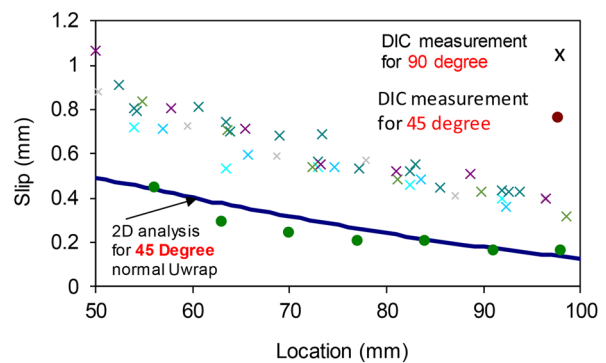
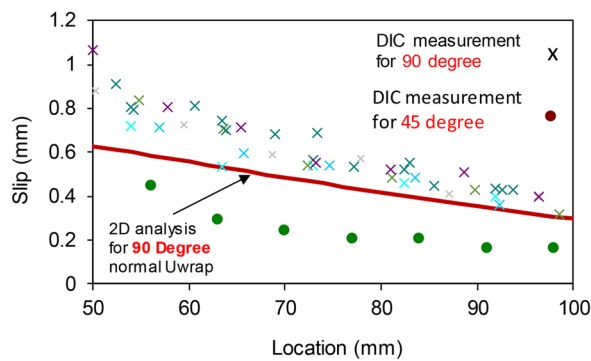
a 2D model vs 3D models (Left: Type 90, Right: Type 45)



b 2D model vs experimental results (Left: Type 90, Right: Type 45)



c Slip profile of 2D model vs 3D model (Left: Type 90, Right: Type 45)



d Slip profile of 2D model vs DIC measurements (Left: Type 90, Right: Type 45)

Fig. 6 Comparison of the 2D model with the 3D model and DIC measurements.

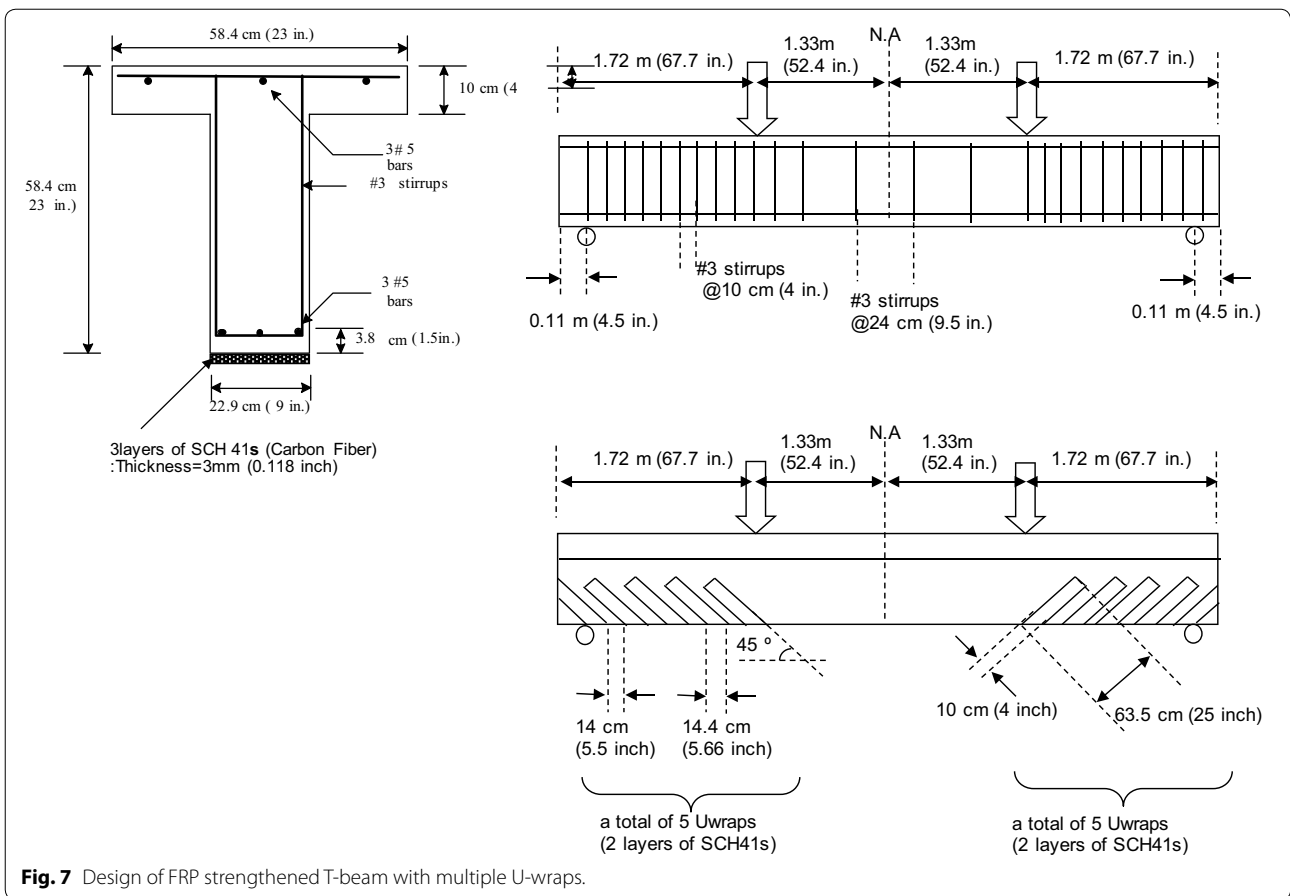


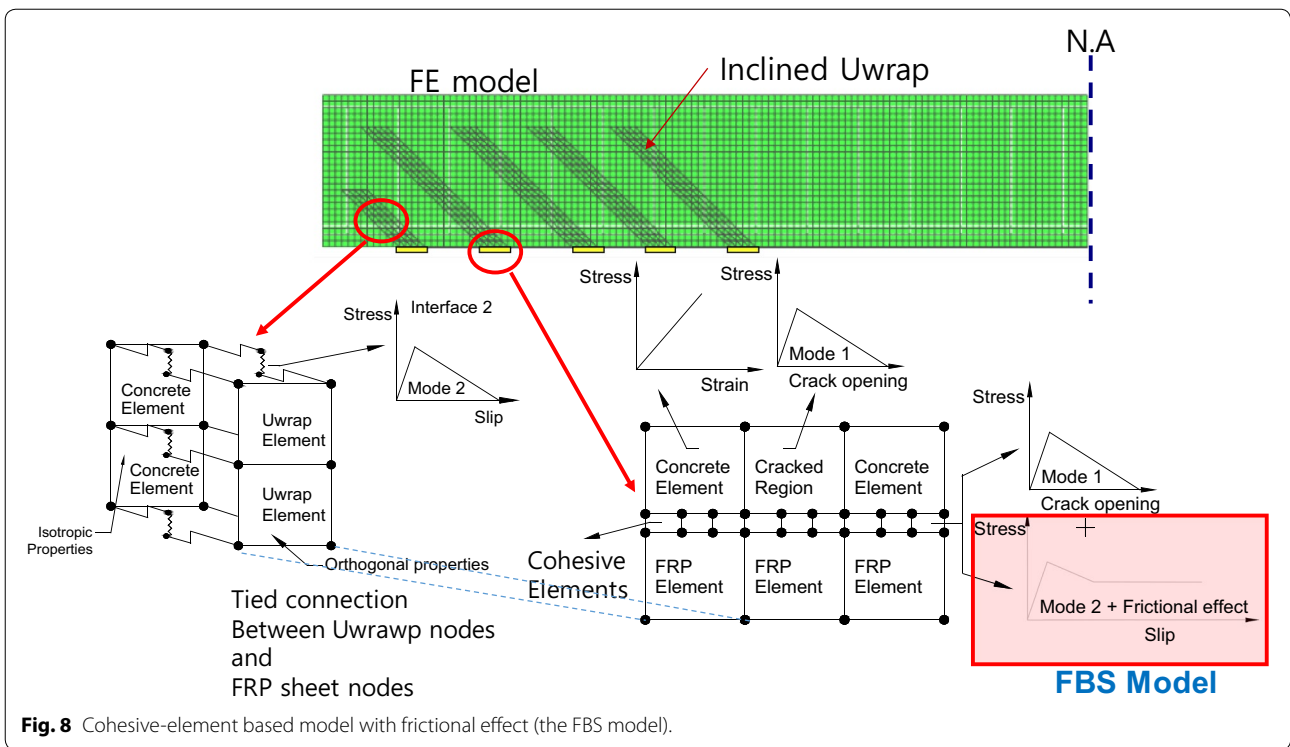
Fig. 7 Design of FRP strengthened T-beam with multiple U-wraps.

found in Lee (2010). To investigate the FBS behavior in the U-wrap region of the beam under flexural load rather than by simple pulling-out load and to observe the maximum anchoring effect simultaneously, the configuration of a 45° U-wrap was selected for strengthening the externally bonded FRP beam. Finally, the obtained results from both the experiment and the model using the FBS were compared. The effectiveness and suitability of using the FBS model will be discussed in a later section.

The element size used for the concrete was 25.4 mm by 25.4 mm. The interface between the FRP and the soffit of the concrete was modeled by cohesive elements. These types of elements were developed to model the behavior of adhesives between two components using the fracture properties, such as Mode 1 and Mode 2 fracture behavior (Hibbitt et al. 2017). The cohesive element size used for the interface between the concrete and the FRP sheet was 1 mm by 1 mm. Since the selected element sizes for concrete and cohesive zone were different, two surfaces with different node spacings were tied. The calculated stress concentration factors were applied to the U-wrap in the 2D model of the large-scale T-beam test following the recommended equations by Campione et al. (2001).

The frictional bond-slip curve for the region under the 45° geometry of the U-wrap was estimated and used as the properties of the cohesive element in Mode 2 behavior. Fig. 8 shows the models developed for the analysis of the large-scale T-beam. The same modeling technique was also used in the previous models of the two T-beams (Lee et al. 2010) except the Mode 2 frictional bond-slip curve in cohesive elements in the U-wrap region. If the all concrete elements were modeled with damaged models, the concrete elements could be damaged even before damage initiation of the cohesive elements. Therefore, the first analysis was done to find the cracked location and patterns inside the concrete beam, and the second analysis was conducted after superimposing the cracked pattern in the concrete beam. The cracked elements from the first analysis were modeled using only the damage plasticity concrete model (Lee and Fenves 1998). The concrete element in non-cracked zone (no damage) was modeled using simple elastic material model.

The orthogonal properties of the U-wrap were also considered using the failure criterion proposed by Hashin and Rotem (1973). The orthogonal properties

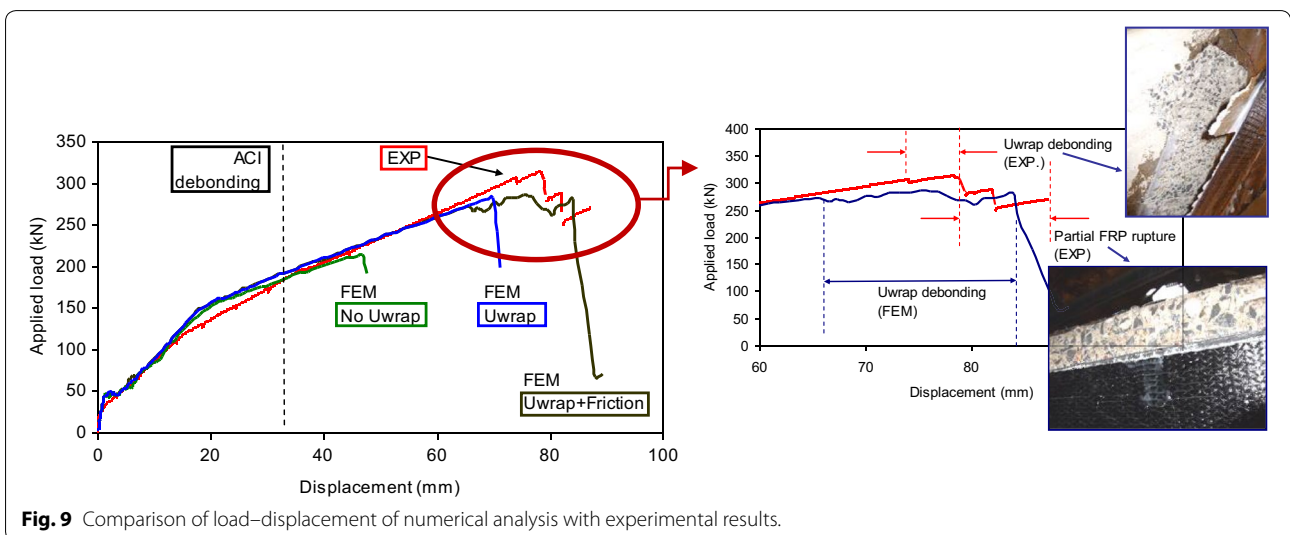


used for the U-wrap in 2D model could be found in Lee et al. (2010). The longitudinal FRP sheet could be modeled with isotropic material properties since it is located in the longitudinal direction in the beam system in 2D model. By contrast, since the U-wrap is deformed in the transverse direction and is attached perpendicular to the axis of the beam length, the transverse tension properties and the shear properties are important parameters of this study. Accordingly, the transverse modulus of elasticity (9.0 GPa), transverse tensile strength (38 MPa) and

shear modulus (1.66 GPa) of the FRP sheet were obtained experimentally.

Figure 9 shows both the experimental and analytical results in one graph. Three simulation results depicting the condition of No-U-wrap, U-wrap without the FBS model and U-wrap with the FBS model were conducted and compared with the experimental results.

As expected, in the simulation results of “without U-wrap”, the FRP sheet debonded much earlier than the experiment. These results showed how effectively the



U-wrap in the numerical models arrested and delayed the debonding propagations between the FRP sheet and the soffit of the concrete beam. The debonding strain of the model without a U-wrap was 0.006, which was close to the calculated debonding strain (0.0056) based on the equation of ACI 440-17. The debonding strain increased almost up to the rupture strain (0.012) when the U-wraps were only considered without the FBS model. Accordingly, additional flexural strengthening effects (33%) were obtained from the addition of the U-wraps. When the frictional behavior was considered (if the FBS model is used), the model showed a more ductile behavior compared to the model with U-wrap and without the FBS model (no friction). The maximum applied load did not increase much due to the frictional effect. However, the final failure took place at a larger mid-span displacement. This indicated that the frictional effects from several U-wraps could delay the debonding propagation, thereby resulting in better ductile behavior. The final failure mode was the debonding of the U-wrap after the debonding of the FRP sheet. The same failure mode was also observed from the experiments. This failure mode is the ideal failure mode for externally bonded FRP system. This is because the rupture of the FRP sheet and rupture of the U-wrap before debonding of the U-wrap can be considered to be a catastrophic failure compared to the more ductile sequence of debonding of the U-wrap after the debonding of the FRP sheet. Even after the debonding of FRP sheet, the U-wrap held the FRP sheet, reducing the brittleness of the failure and resulting in a better ductile behavior. This ductile behavior could prevent one of the major disadvantages of the externally bonded FRP system, the brittle failure. This indicates that the safety issue and the conservative nature of FRP design code regarding the externally bonded FRP system (ACI 440-17) can be improved with appropriate U-wrap design.

Figure 10 shows both the experimental and numerical strain values along the longitudinal axis of the FRP. The results showed that the strain distributions along the longitudinal FRP sheet were well predicted at every load level. It is also interesting to note that the strain at non-U-wrap locations displayed a plateau, while the strain at the U-wrap locations showed variations along the length of the FRP sheet. It was thought that since the area between the U-wraps was already debonded, the unbonded behavior between the adjacent U-wraps appeared as plateau in the graph.

The experimentally obtained strains from several U-wraps during the flexural behavior of the strengthened T-beam was compared with the results from the developed numerical analysis (see Fig. 11). The experimentally obtained strains from the U-wrap were averaged from both sides of the beam and compared with

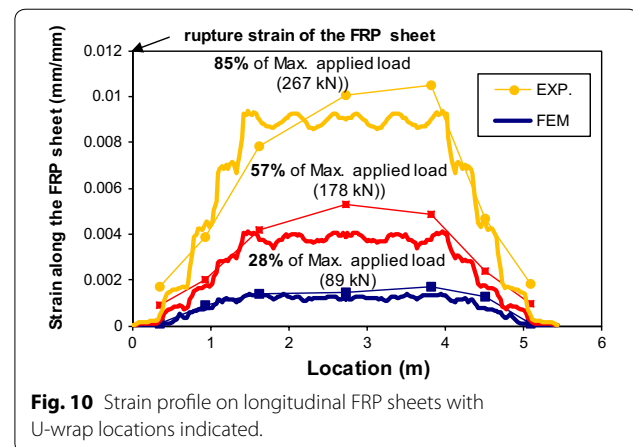
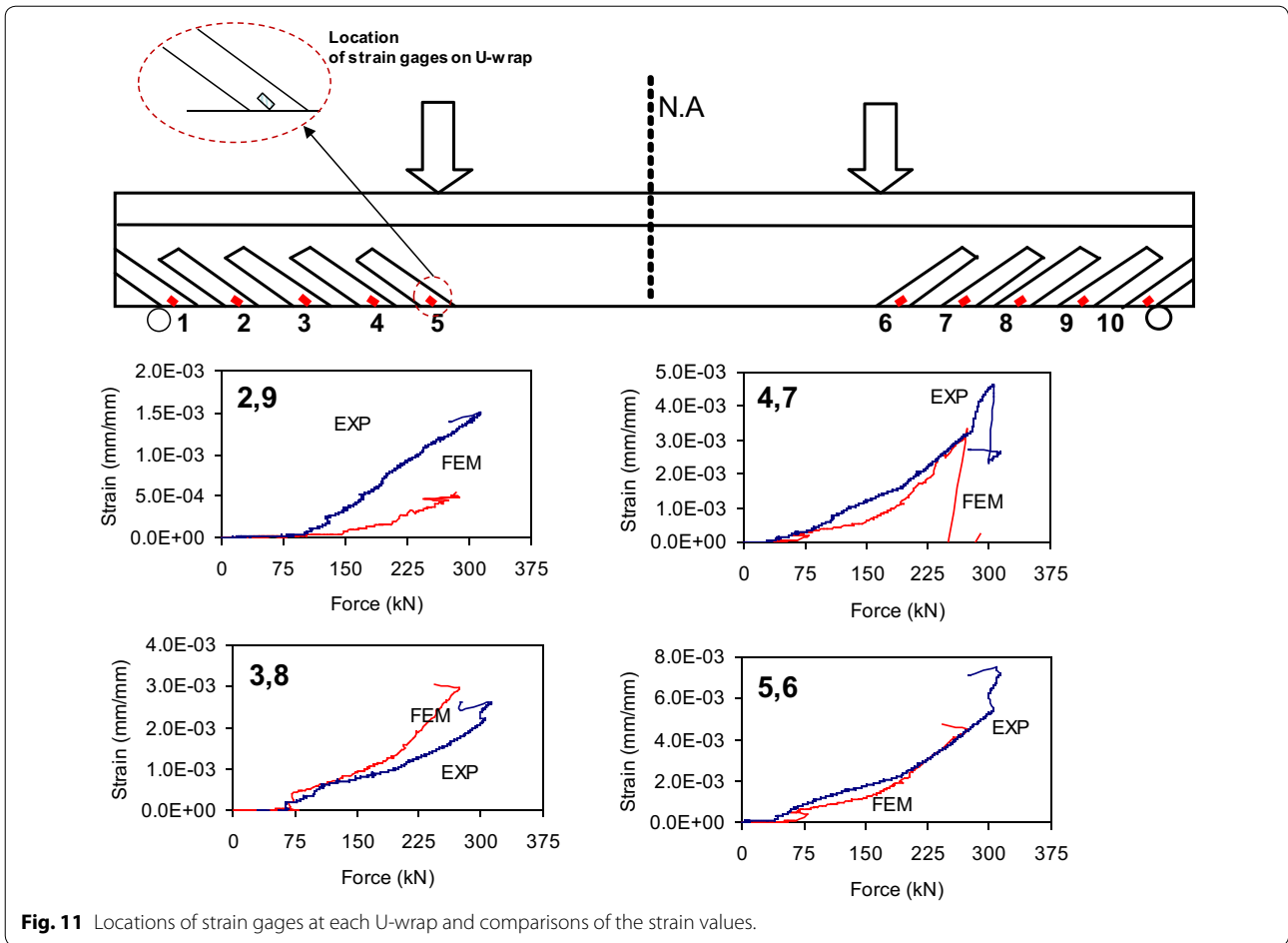


Fig. 10 Strain profile on longitudinal FRP sheets with U-wrap locations indicated.

the results of axis-symmetric numerical models. Experimentally, it was observed that the debonding propagated from the mid-span toward the anchor zone, and one of the U-wraps was debonded before localized failure of the FRP due to rupture. This indicated that the transferred load from the strained FRP sheet was beyond the limitation of the anchor capacity of the U-wraps. Accordingly, the magnitudes of strain in the U-wrap (0.0015–0.007) obtained from this test were much larger than that obtained from the previous two T-beams (0.00008–0.001) (Lee et al. 2010), indicating that the tested T-beam in the current study was under much larger anchoring effects. In Fig. 11 each location of the strain gage could be found. As shown in Fig. 11, U-wrap 4 through U-wrap 7 were activated. It should be noted that U-wrap 6 was debonded due to the significantly strained FRP sheet in its vicinity. The U-wraps near the supports showed a small level of strain, which indicated that the U-wraps at those locations were not activated as anchors. The U-wraps (U5 and U6) near the loading point showed five times larger strain than the U-wraps (U1 and U10) near the supports. These trends were well captured by our developed models. The levels of strain at each U-wrap were well predicted. The two U-wraps (U1 and U10) which were close to the supports were not predicted accurately by the models since they were in the disturbed regions (D-regions). However, the overall trends were predicted satisfactorily.

In the test, it was observed that U-wrap 6 (U6) was completely debonded, and U-wrap 5 (U5) was about to be debonded. The rest of the U-wraps did not completely debonded before the rupture of the longitudinal FRP sheet. Had the FRP sheet not been fractured, the rest of the U-wraps would have also been completely debonded. On the other hand, in the numerical analysis, the failure mode obtained was the debonding of



all the U-wraps before the rupture of the FRP. When the U-wraps were debonded in the numerical analysis, the strain of the FRP sheet at mid-span was 0.0115. However, the rupture strain in the numerical analysis was set to 0.012. This indicated that the test condition was close to the balanced condition between the debonding of the U-wrap and the rupture of the FRP sheet. Accordingly, in the numerical models, all the U-wraps were debonded before the rupture of the FRP sheet. However, experimentally, some of the U-wraps were debonded, followed by partial rupture of the FRP sheet. This was due to the local stress concentration effect along the FRP sheet before all the U-wraps were debonded.

7 A Comparison of Debonding Strain Values at Longitudinal FRP Sheet with U-wraps

The debonding strain of the longitudinal FRP sheet is an important parameter for comparing the anchoring effects of the U-wrap configuration. As ACI 440-2R (2017) indicated, every design done for externally bonded FRP

system should be based on estimated debonding strain of the longitudinal FRP sheet (ϵ_{fd}). Therefore, in this section, the debonding strain of the longitudinal FRP sheet from both the experiment and the FBS model will be compared, as shown in Fig. 12a. From the experiment of T-beam with 45° inclined U-wraps in the current study, ϵ_{fd} was 1150 $\mu\epsilon$, whereas the obtained result based on the FBS model showed 1075 $\mu\epsilon$. The variation of applied load with FRP strain curves was also well predicted. Therefore, the debonding strain due to the addition of U-wrap could be predicted satisfactorily within a margin of 8.0% error. The developed FBS model was also applied to the results of other comparable studies (Fu et al. 2016) for additional verifications. For that study, three different configurations were considered and models were developed following the FBS model. Both V1L1W60 and V2L2W60 indicated 90° U-wrap (vertical U-wrap with no inclination). The other beam, I1L1W90 referred to a 45° inclined U-wrap. The detailed geometries can be found in Fu et al. (2016). The obtained results using the FBS model for three different configurations, V1L1W60, V2L1W60, I1L1W90 were

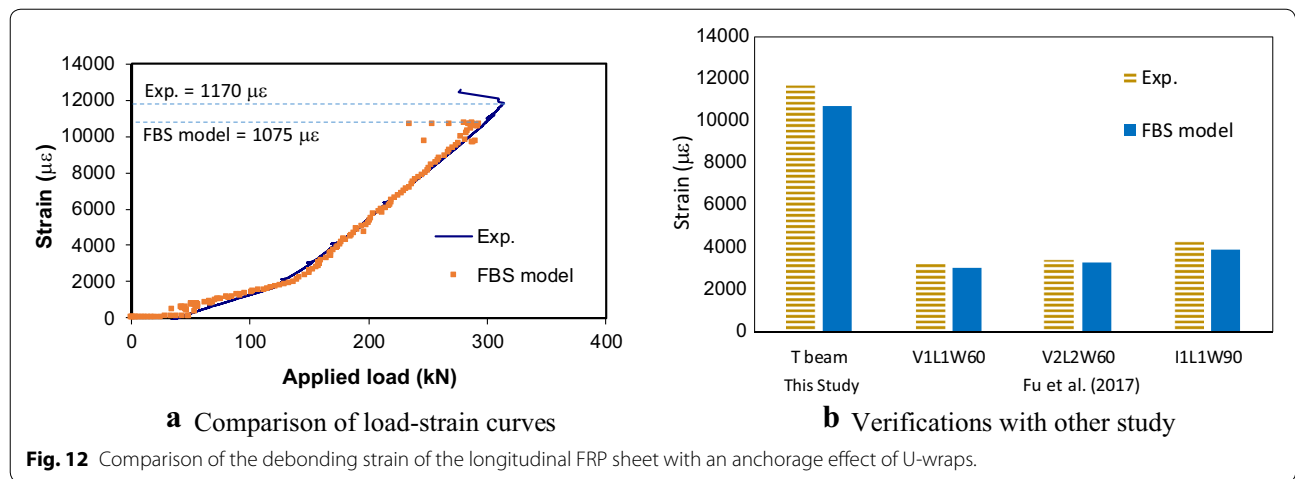


Table 1 Model description for parametric study.

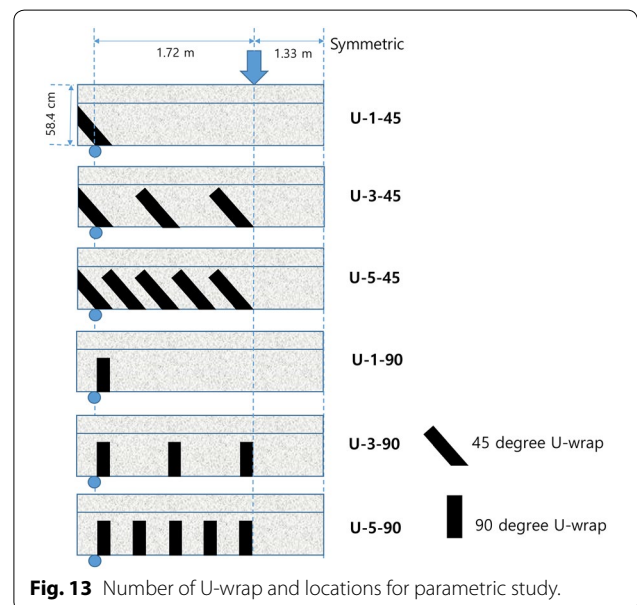
Specimen	Angle of U-wrap	Number of U-wrap	Layers of FRP sheet	FBS model
No U-wrap	NA	NA	3	X
U-1-45	45	1	3	O
U-3-45	45	3	3	O
U-5-45	45	5	3	O
U-1-90	90	1	3	O
U-3-90	90	3	3	O
U-5-90	90	5	3	O

3040, 3313 and 3920 $\mu\epsilon$, respectively, while the obtained experimental results were 3258, 3472 and 4292 $\mu\epsilon$, respectively, as shown in Fig. 12b. The average absolute different ratios were calculated to be 7% when the FBS model was used to predict the debonding strain of the longitudinal FRP sheet. The obtained results indicated that the frictional effect after debonding between the FRP and soffit of the concrete are the key parameters to consider when a U-wrap is used for anchoring effects.

8 Parametric Study of the Externally Bonded FRP Beam with U-wrap

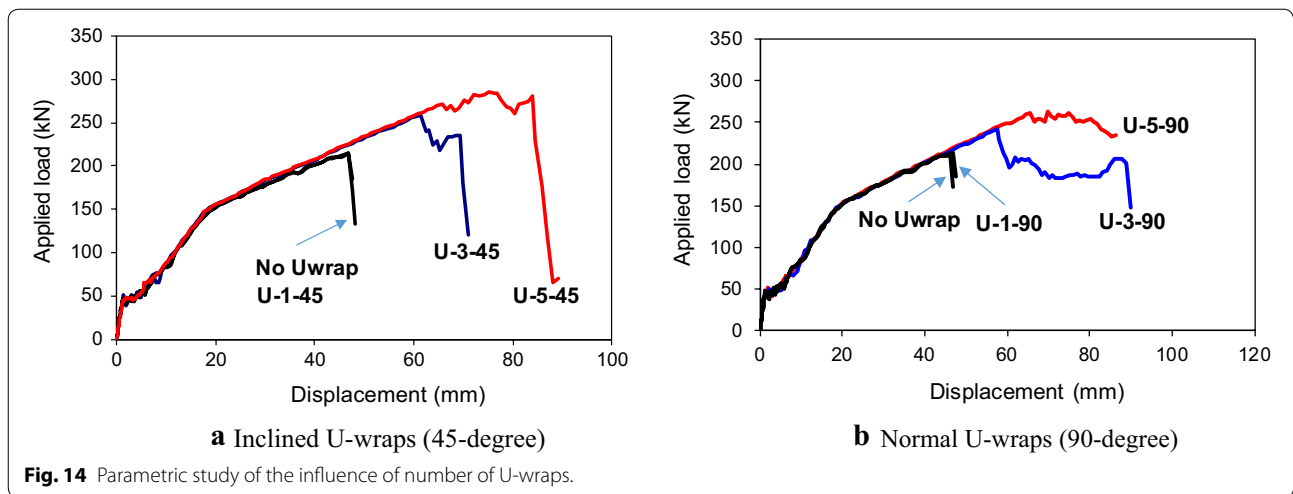
After conducting the model verifications, a parametric study was performed in order to understand the effects of the numbers and angle of U-wrap in the load–displacement behavior. A total of six different cases were considered based on two parameters, viz. the number of U-wraps and the angle of U-wrap. The details of the 6 cases have been summarized in Table 1. Specimen nomenclature was named as U-“number of U-wraps”-“angle of U-wrap”.

The specific locations of the U-wraps are shown in Fig. 13. The same moment span and shear span were used for this parametric study. The distance between



the two adjacent U-wraps were kept the same and symmetric about the neutral axis. The specific geometries of the 45- and 90° U-wraps and the distances between the U-wraps can be found from Fig. 7 since the spacing between the U-wraps was constant.

Figure 14a shows the obtained load–displacement graph from 45° U-wraps. The load displacement graphs were obtained from the loading point shown in Fig. 13. The results indicated that an increasing number of U-wraps can delay the debonding propagation of the FRP sheet. However, the models for No-U-wrap and U-1-45 showed a similar behavior. This indicated that if the anchor capacity of the U-wrap is not enough, the U-wraps could not carry the load from the released strain energy generated from the debonding of the FRP

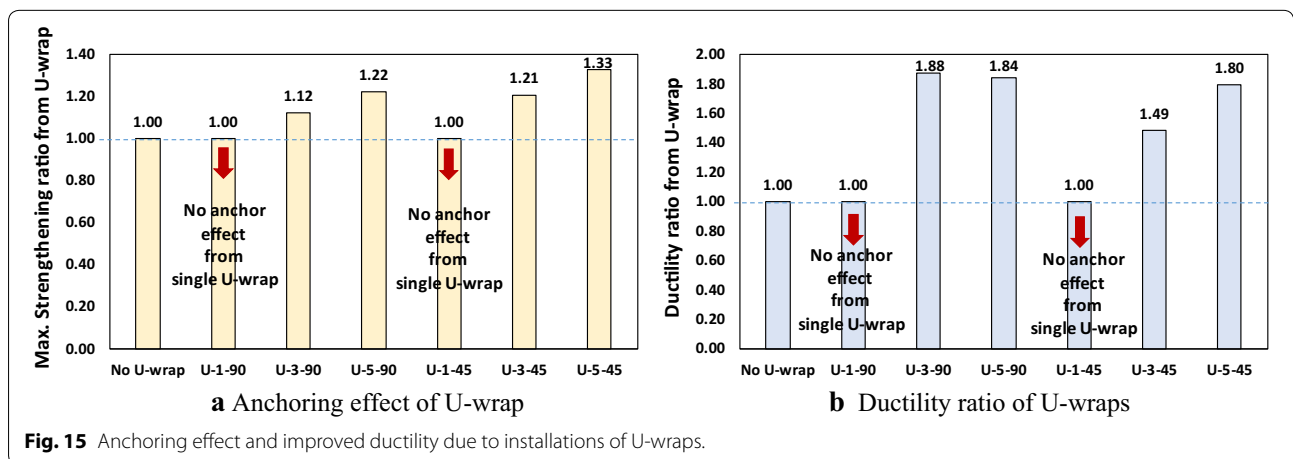


sheet. This released energy generated from the debonding of the FRP sheet could be arrested by installing more anchors (U-wraps) intermittently. This is the reason why the U-1-45 showed the same behavior as that of the No-U-wrap, while U-3-45 and U-5-45 showed increments in the maximum loads and maximum displacements in comparison with the No U-wrap. Furthermore, the ductile behavior was obtained from both the U-3-45 and U-5-45 as the debonding propagation was delayed due to anchoring effect of the U-wraps, indicating that ductility of the externally strengthened concrete structure with FRP sheet could be improved by adding more U-wraps.

Figure 14b shows the load–displacement graph from the 90° U-wraps. A 90° U-wrap could allow more slips than a 45° U-wrap. The shear strained 90° unidirectional U-wrap allowed much larger displacement than the tensile strained 45° U-wrap. However, the strengthening effects were smaller than that of the 45° U-wrap. For

the 45° U-wrap, the tensile strain in the fiber was more active than the shear strain, and so, the anchoring effects could be maximized. Therefore, the strengthening effects obtained from the U-3-90 and U-5-90 were less than that obtained from the U-3-45 and U-5-45. However, the ductility of U-3-90 increased more than that of the U-3-45 as there was an increase in the maximum displacement.

Figure 15 shows the obtained anchoring effect and improved ductility due to the installation of the U-wrap. The applied load and displacement at debonding failure without U-wrap were 214.9 kN and 46.8 mm, respectively. Accordingly, strengthening ratios due to the anchoring effects of the U-wraps are summarized as shown in Fig. 15(a). The maximum strengthening ratio due to addition of the U-wraps was 33% for U-5-45. It was also found that the ductility ratio could also be improved significantly as the more U-wraps were installed, as shown in Fig. 15(b). The ductility ratio was calculated as a displacement at ultimate debonding of the FRP sheet



divided by a displacement without U-wrap. The maximum improvement in the ductility ratio obtained from this study was 88% from U-3-90.

Based on the parametric study, some important conclusions can be derived. First, there is a threshold value for the number of effective U-wrap. As observed in this research, one anchor was not sufficient to carry the sudden release of the strain from the FRP sheet. For this study, three U-wraps could effectively arrest or delay the debonding propagation of the FRP sheet. Second, the number of U-wraps installed intermittently could effectively delay the debonding propagation from the loading points to the supports. Third, better ductile behavior could be obtained from the 90° U-wraps. However, for maximizing the strengthening effects, a 45° U-wrap was a better choice. To sum up, the ductile behavior of the RC beam with externally bonded FRP sheet could be controlled by using various U-wrap designs.

9 Conclusion and Principal Findings

The frictional bond-slip (FBS) model was developed for the first time (Lee 2010) and applied to the concrete blocks with attached FRP sheets (Lee and Lopez 2019). In this present study, that model was also applied to model large-scaled RC beams and was further verified with experimental results. Analytical models were developed to evaluate the effect of the U-wrap on the externally bonded FRP system using the FBS model and the fracture mechanics (Mode I and Mode II fracture energy). Based on the obtained results from the 3D models of the pull-out specimens, more efficient 2D models were developed using the FBS model and cohesive elements which also considered both mode I and II fracture energy. The developed 2D model was compared with 3D model as well as the experimental results from other studies (Fu et al. 2016) for verifications. These findings were used to successfully predict the behavior of a large scale FRP strengthened beam with various U-wrap designs. The following conclusions were derived from the numerical study.

- a. The developed 2D model using the FBS model accurately predicted the increased debonding strengthening effect, slip profiles and frictional effect of pull-out specimens in the U-wrap region.
- b. The developed analytical 2D model using the FBS model (Lee and Lopez 2019) with orthogonal properties of the U-wrap was able to predict the flexural capacity and strain of the FRP sheet at debonding. The model also predicted the sequences of the experimental failure modes of a large scale FRP strengthened T-beam with U-wraps.
- c. Strain distributions in the FRP sheets were well predicted by the 2D analytical models with 7% of an average absolute different ratio. The use of the FBS model with cohesive elements added the capability of capturing the anchoring effects in the U-wrap regions.
- d. The ductile behavior obtained from the use of U-wraps as anchorage for the FRP longitudinal sheets could prevent one of the major disadvantages of the externally bonded FRP system, viz. the brittle debonding failure. This results indicates that the current ACI FRP design guideline regarding the externally bonded FRP system (ACI 440-17) could recommend appropriately designed U-wraps in order to reduce the likelihood of brittle failure modes.
- e. In the modeling of the T-beam with the U-wraps for anchoring effect, additional flexural strengthening capacity (33%) was obtained due to the addition of the U-wraps (45°).
- f. Results showed that if the installed U-wrap had less capacity than the threshold value defined by the analysis, the U-wrap could not carry the load from the released strain energy generated from the debonding of the FRP sheet, thereby resulting in a no-anchor effect.
- g. Multiple U-wraps more than three effectively delayed the debonding between FRP and soffit of the concrete. However, it should be mentioned that the effective number of U-wrap for delaying debonding is dependent to beam geometries and loading conditions. It was confirmed by this study that a better ductile behavior was obtained from the multiple use of 90° U-wrap. However, for the goal of maximizing the strengthening effects, a 45° U-wraps would be the better choice.
- h. The ductile behavior of the RC beam with externally bonded FRP sheet was obtained by using various types of U-wrap designs. In this study, an 88% improvement in ductility was obtained using the 90° U-wraps.

Acknowledgements

This research was supported by Basic Science Research Program through the National Research Foundation of Korea (NRF), funded by the Ministry of Science and ICT (2018R1A1A1A05018602) and a CAREER Grant from the National Science Foundation (CMS-0330592). The authors greatly acknowledge these supports.

Authors' contributions

JL conceived of the presented idea, developed the numerical models, conducted experiments and computations and wrote the manuscript. ML designed the experimental program and supervised the entire project. All authors provided critical feedback and helped shape the research, analysis and manuscript. Both authors read and approved the final manuscript.

Funding

Ministry of Science and ICT (2018R1A1A1A05018602) and a CAREER Grant from the National Science Foundation (CMS-0330592).

Availability of data and materials

Not applicable

Competing interests

The authors declare that they have no competing interests.

Author details

¹ Department of Civil Engineering, National Korea Maritime and Ocean University, 609 Engineering Building-II, Busan 606-791, South Korea. ² MODJESKI and MASTERS, Inc., 100 Sterling Parkway, Suite 302, Mechanicsburg, PA 17050, USA.

Received: 21 June 2019 Accepted: 28 October 2019

Published online: 07 January 2020

References

- ACI Committee 440. (2017). *Guide for the design and construction of externally bonded FRP systems for strengthening concrete structures*. Farmington Hill, MI: ACI 440.2R-17, American Concrete Institute.
- ASTM. (2005). *Standard test method for compressive strength of cylindrical concrete specimens*. West Conshohocken, PA: ASTM C39.
- ASTM. (2011). *Standard test method for splitting tensile strength of cylindrical concrete specimens*. West Conshohocken, PA: ASTM C496.
- ASTM. (2012). *Standard test method for shear properties of composite materials by the V-Notched beam method*. West Conshohocken, PA: ASTM D5379.
- ASTM. (2014). *Standard test method for tensile properties of polymer matrix composite materials*. West Conshohocken, PA: ASTM D3039.
- Baky, H. A., Ebead, U. A., & Neale, K. W. (2012). Nonlinear micromechanics-based bond-slip model for FRP/concrete interfaces. *Engineering Structures*, *39*, 11–23.
- Brena, S. F., Bramblett, R. M., Wood, S. L., & Kreger, M. E. (2003). Increasing flexural capacity of reinforced concrete beams using carbon fiber-reinforced polymer composites. *ACI Structural Journal*, *100*(1), 36–46.
- Campione, G., Miraglia, N., & Scibilia, N. (2001). Compressive behaviour of RC members strengthened with carbon fibre reinforced plastic layers. *Advanced Earthquake Engineering*, *2001*, 397–406.
- Chen, J., & Teng, J. (2001). Anchorage strength models for FRP and steel plates bonded to concrete. *Journal of the Structural Engineering. American Society of Civil Engineers*, *127*(7), 784–791.
- Fu, B., Teng, J. G., Chen, J. F., Chen, G. M., & Guo, Y. C. (2016). Concrete cover separation in FRP-plated RC beams: mitigation using FRP U-jackets. *Journal of Composites for Construction*, *21*(2), 04016077.
- Grelle, J. V., & Sneed, L. H. (2013). Review of anchorage systems for externally bonded FRP laminates. *International Journal of Concrete Structures and Materials*, *7*(1), 17–33.
- Hashin, Z., & Rotem, A. (1973). Fatigue failure criterion for fiber reinforced materials. *Journal of Composite Materials*, *7*, 448–464.
- Hibbitt Karlsson and Sorenson Inc. (2017). *ABAQUS/Explicit: user's manual*. Pawtucket, RI: Hibbitt Karlsson and Sorenson Inc.
- Khalifa, E. S., & Al-tersawy, S. H. (2013). Experimental and analytical investigation for enhancement of flexural beams using multilayer wraps. *Composites Part B Engineering*, *45*(1), 1359–8368.
- Kishi, N., Zhang, G., & Mikami, H. (2005). Numerical cracking and debonding analysis of RC beams reinforced with FRP sheet. *Journal of Composites for Construction*, *9*(6), 507–514.
- Kotynia, R., Baky, H. A., Neale, K. W., & Ebead, U. A. (2008). Flexural strengthening of RC beams with externally bonded CFRP systems: Test results and 3D nonlinear FE analysis. *Journal of Composites for Construction*, *12*(2), 190–201.
- Lee, J. H. (2010). Performance of U-wrap as an anchorage system in externally bonded FRP reinforced concrete elements. Ph.D. Thesis, The Pennsylvania State Univ., University Park, USA
- Lee, J. H., Chacko, R. M., & Lopez, M. M. (2010). Use of mixed mode fracture interfaces for the modeling of large scale FRP strengthened beams. *ASCE Journal of Composite for Construction*, *14*(6), 845–855.
- Lee, J., & Fenves, G. L. (1998). Plastic-damage model for cyclic loading of concrete structures. *Journal of engineering mechanics*, *124*(8), 892–900.
- Lee, J. H., & Lopez, M. M. (2011). *Non-contact measuring techniques to characterize deformation on FRP U-wrap anchors* (p. 275). Farmington Hill, MI: ACI Special Publication.
- Lee, J., & Lopez, M. M. (2016). Characterization of FRP U-wrap anchors for externally bonded FRP reinforced concrete elements—an experimental study. *ASCE Journal of Composite for Construction*, *20*(4), 4016012.
- Lee, J., & Lopez, M. M. (2019). Frictional bond-slip model for the concrete-FRP interface under the FRP U-wrap region. *Construction and Building Materials*, *194*, 226–237.
- Lee, J. H., Lopez, M. M., & Bakis, C. E. (2009). Slip effects in reinforced concrete beams with mechanically fastened FRP strip. *Cement Concrete Composites*, *31*(7), 496–504.
- Niu, H., Karbhari, V. M., & Wu, Z. (2006). Diagonal macro-crack induced debonding mechanisms in FRP rehabilitated concrete. *Composites Part B Engineering*, *37*(7–8), 627–641.
- Ozbakkaloglu, T., & Saatcioglu, M. (2009). Tensile behavior of FRP anchors in concrete. *Journal of Composites for Construction*, *13*(2), 1272–1279.
- Triantafyllou, T. C. (1998). Shear strengthening of reinforced concrete beams using epoxy bonded FRP composites. *ACI Structural Journal*, *95*(2), 107–115.
- Wang, J. (2007). Cohesive zone model of FRP-concrete interface debonding under mixed-mode loading. *International Journal of Solids and Structures*, *44*(20), 6551–6568.
- Wang, J., & Zhang, C. (2008). Nonlinear fracture mechanics of flexural-shear crack induced debonding of FRP strengthened concrete beams. *International Journal of Solids and Structures*, *45*(10), 2916–2936.
- Yuan, H., Teng, J. G., Seracino, R., Wu, Z. S., & Yao, J. (2004). Full-range behavior of FRP-to-concrete bonded joints. *Engineering Structures*, *26*(5), 553–565.
- Zhang, H. W., & Smith, S. T. (2012). FRP-to-concrete joint assemblages anchored with multiple FRP anchors. *Composite Structures*, *94*(2), 403–414.

Publisher's Note

Springer Nature remains neutral with regard to jurisdictional claims in published maps and institutional affiliations.